



Dark photon production via $\gamma\gamma \rightarrow \gamma A'$

Xiaorui Wong^{1,2,a} , Yongsheng Huang^{2,b}

¹ School of Physics, Peking University, Beijing 100871, China

² Institute of High Energy Physics, Chinese Academy of Sciences, Beijing 100049, China

Received: 6 April 2021 / Accepted: 10 May 2021 / Published online: 23 May 2021
© The Author(s) 2021

Abstract The dark photon is a new gauge boson which arises from an extra $U'(1)$ gauge symmetry. In this paper, a novel dark photon production mechanism based on MeV-scale $\gamma\text{-}\gamma$ collider is considered: $\gamma\gamma \rightarrow \gamma A'$. With the aid of PACKAGE-X, differential cross section of $\gamma\gamma \rightarrow \gamma A'$ is obtained, as a function of the kinetic mixing parameter ε and dark photon mass $m_{A'}$. Taking the light-by-light scattering as background, the constraints on the dark photon parameter space for different time intervals in a MeV-scale $\gamma\text{-}\gamma$ collider are also given.

1 Introduction

The dark matter problem has never lost its allure for nearly a century [1–4]. Back to 1922, Jacobus Kapteyn first suggested the existence of dark matter by stellar velocities [5]. In 1933, Fritz Zwicky postulated dark matter by the huge discrepancies between luminous mass and dynamical mass of the Coma Cluster [6]. There are many observational evidences for dark matter in cosmology: galaxy rotation curve [7–9], gravitational lensing [10, 11], bullet cluster [12], cosmic microwave background [13, 14] and so on.

Dark matter candidates include: weakly interacting massive particles (WIMPs), asymmetric dark matter, axions, sterile neutrinos, dark photon, etc. WIMPs are expected to have been thermally produced in the early universe, they have large mass compared to standard particles, and they interact with cross sections no higher than the weak scale [15]. Models of asymmetric dark matter are based on the idea that dark matter may carry a matter-antimatter asymmetry [16]. The existence of axions was first postulated to solve the strong CP problem of quantum chromodynamics (QCD) [17]. Sterile neutrinos are neutrinos with right-handed chirality, and they interact only via gravity [18].

Dark photon is the gauge boson of an extra $U'(1)$ symmetry [19], and can interact with Standard Model photon via kinetic mixing [20–22]. Dark photon could be either massless or massive in different frames. The massive case has gained a lot of attention because it couples directly to the standard model currents and is more readily accessible in experiment [23]. In this work, massive dark photon is considered.

The production mechanisms of dark photon mainly include: bremsstrahlung [24], annihilation [25–27], meson decay [28] and Drell–Yan [29]. Many related experiments [30–42] have been taken. But still, no robust signature of dark photon has come out.

In this paper, a novel dark photon production mechanism based on $\gamma\text{-}\gamma$ collider is considered: $\gamma\gamma \rightarrow \gamma A'$. Where γ means standard model photon and A' stands for dark photon. $\gamma\text{-}\gamma$ collider was firstly suggested in the early 1980s, with a concept of creating it by uniting linear electron accelerators with high peak and average power lasers [43]. There is still no $\gamma\text{-}\gamma$ colliders in the world, but the technology of building a MeV-scale $\gamma\text{-}\gamma$ collider is being mature. Furthermore, the background is respectively clean, which could serve better environment in searching dark photon. In this paper, differential cross section of the process $\gamma\gamma \rightarrow \gamma A'$ is calculated and limits on dark photon parameter space in a $\gamma\text{-}\gamma$ collider are also given.

This paper is organized as follows: in Sect. 2, the dark photon model will be given, and amplitude of $\gamma\gamma \rightarrow \gamma A'$ is calculated. In Sect. 3, we analyse our results and gave limits on dark photon in a MeV-scale $\gamma\text{-}\gamma$ collider. Finally, summary is made in Sect. 4.

2 Amplitude of $\gamma\gamma \rightarrow \gamma A'$

If the Standard Model gauge group is extended by adding a new abelian $U'(1)$ symmetry: $SU(3) \times SU(2) \times U(1) \times U'(1)$, a corresponding new gauge vector boson will occur, which is called dark photon and often labeled by A' or γ' .

^a e-mail: xiaorui_wong@pku.edu.cn

^b e-mail: huangys82@ihep.ac.cn (corresponding author)

With two $U(1)$ s in the gauge group, there will be kinetic mixing, the mixing term can be written as [21]:

$$\mathcal{L}_{mix} = -\frac{\varepsilon}{2} F_{\mu\nu} F'^{\mu\nu}. \tag{1}$$

The Lagrangian is:

$$\mathcal{L} = -\frac{1}{4} F_{\mu\nu} F^{\mu\nu} - \frac{1}{4} F'_{\mu\nu} F'^{\mu\nu} - \frac{\varepsilon}{2} F_{\mu\nu} F'^{\mu\nu} + \frac{1}{2} m_{A'}^2 V_\mu V^\mu \tag{2}$$

where ε is kinetic mixing parameter, $m_{A'}$ is mass of dark photon, ε and $m_{A'}$ are the only two free parameters. $F_{\mu\nu}$ is the field strength tensor of $U(1)$ and $F'_{\mu\nu} = \partial_\mu V_\nu - \partial_\nu V_\mu$ is the field strength tensor of $U'(1)$.

Dark photon production is considered via $\gamma\gamma \rightarrow \gamma A'$, this reaction can be taken as the result of the production of a virtual electron–positron pair by two initial photons,

$$\Pi_s^{\mu\rho\nu\lambda} = -\beta^{2\varepsilon} \int \frac{d^n p}{(2\pi)^n} \frac{\text{tr}[\gamma^\mu(\not{p} + m)\gamma^\nu(\not{p} + \not{k}_3 + m)\gamma^\lambda(\not{p} + \not{k}_1 + \not{k}_2 + m)\gamma^\rho(\not{p} + \not{k}_1 + m)]}{(p^2 - m^2 + i0^+)[(p + k_3)^2 - m^2 + i0^+][(p + k_1 + k_2)^2 - m^2 + i0^+][(p + k_1)^2 - m^2 + i0^+]} \tag{7}$$

followed by annihilation of the pair into the final state photon, and the dark photon.

Define k_1 and k_2 are momentums of incoming photons, k_3 is momentum of outgoing photon and k_4 is momentum of outgoing dark photon:

$$\begin{aligned} k_1 &= (\omega, 0, 0, \omega) \\ k_2 &= (\omega, 0, 0, -\omega) \\ k_3 &= (|\mathbf{k}_3|, |\mathbf{k}_3| \sin \theta, 0, |\mathbf{k}_3| \cos \theta) \\ k_4 &= (\sqrt{m_{A'}^2 + |\mathbf{k}_3|^2}, -|\mathbf{k}_3| \sin \theta, 0, -|\mathbf{k}_3| \cos \theta) \end{aligned}$$

$\hbar\omega$ is energy of an incoming photon, here we set $\hbar = 1$. θ is the angle between directions of outgoing and incoming photons.

We define Mandelstam variable:

$$s = (k_1 + k_2)^2, t = (k_1 - k_3)^2, u = (k_1 - k_4)^2 \tag{3}$$

which satisfies:

$$s + t + u = m_{A'}^2. \tag{4}$$

Differential cross section of this process is:

$$\frac{d\sigma}{d\Omega} = \frac{1}{64\pi^2(4\omega)^2} \frac{|\mathbf{k}_3|}{|\mathbf{k}_1|} |\mathcal{M}_{\text{fi}}|^2. \tag{5}$$

Because $k_1 + k_2 = k_3 + k_4$, it is easy to get $\frac{|\mathbf{k}_3|}{|\mathbf{k}_1|} = 1 - \frac{m_{A'}^2}{s}$.

The amplitude of $\gamma\gamma \rightarrow \gamma A'$ has contributions from six diagrams. Three are shown in Fig. 1, the other three differ from these only in that the internal electron loop traverses in the opposite direction. Amplitude of the diagram with clockwise direction of electrons in the loop is the same as that with the anticlockwise direction loop, so the total scattering amplitude is:

$$i\mathcal{M}_{\text{fi}} = 2\varepsilon e^4 (\Pi_s^{\mu\rho\nu\lambda} + \Pi_t^{\mu\rho\nu\lambda} + \Pi_u^{\mu\rho\nu\lambda}) \epsilon_\mu(k_1) \epsilon_\rho(k_2) \epsilon_\nu^*(k_3) \epsilon_\lambda'^*(k_4) \tag{6}$$

where $\epsilon_\mu(k_1), \epsilon_\rho(k_2)$ are polarisation vectors of incoming photons, $\epsilon_\nu^*(k_3), \epsilon_\lambda'^*(k_4)$ are polarisation vectors of outgoing photon and dark photon, $\Pi_s^{\mu\rho\nu\lambda}, \Pi_t^{\mu\rho\nu\lambda}, \Pi_u^{\mu\rho\nu\lambda}$ are loop contributions of diagrams (s), (t), (u) in Fig. 1.

From quantum field theory, we can get:

where m is electron mass, β is an introduced parameter to make the dimension correct, $\epsilon = \frac{4-n}{2}$. $\Pi_t^{\mu\rho\nu\lambda}$ and $\Pi_u^{\mu\rho\nu\lambda}$ can be got similarly.

Amplitudes are calculated with PACKAGE-X [44]. Each diagram in Fig. 1 has divergent contribution, as shown in Eqs. (8)–(10) respectively:

$$\frac{4g^{\lambda\nu}g^{\mu\rho}}{3\epsilon} + \frac{4g^{\lambda\rho}g^{\mu\nu}}{3\epsilon} - \frac{8g^{\lambda\mu}g^{\rho\nu}}{3\epsilon} \tag{8}$$

$$- \frac{8g^{\lambda\nu}g^{\mu\rho}}{3\epsilon} + \frac{4g^{\lambda\rho}g^{\mu\nu}}{3\epsilon} + \frac{4g^{\lambda\mu}g^{\rho\nu}}{3\epsilon} \tag{9}$$

$$\frac{4g^{\lambda\nu}g^{\mu\rho}}{3\epsilon} - \frac{8g^{\lambda\rho}g^{\mu\nu}}{3\epsilon} + \frac{4g^{\lambda\mu}g^{\rho\nu}}{3\epsilon}. \tag{10}$$

The metric tensor $g^{\mu\nu} = \text{diag}\{1, -1, -1, -1\}$. It is obviously to tell total amplitude has a finite result.

Under low energy limit, taking the $n \rightarrow 4$, the full loop contribution reads as:

$$\begin{aligned} \Pi^{\mu\rho\nu\lambda} &= \Pi_s^{\mu\rho\nu\lambda} + \Pi_t^{\mu\rho\nu\lambda} + \Pi_u^{\mu\rho\nu\lambda} \\ &= \frac{1}{m^4} \left[\frac{4}{15} k_1^\rho k_1^\nu k_2^\mu k_3^\lambda + \frac{4}{15} k_1^\rho k_2^\mu k_2^\nu k_3^\lambda + \frac{4}{15} k_1^\rho k_1^\nu k_2^\lambda k_3^\mu \right. \\ &\quad - \frac{28}{45} k_1^\lambda k_1^\rho k_2^\nu k_3^\mu - \frac{28}{45} k_1^\rho k_2^\lambda k_2^\nu k_3^\mu \\ &\quad + \frac{28}{45} k_1^\rho k_2^\nu k_3^\lambda k_3^\mu - \frac{28}{45} k_1^\lambda k_1^\nu k_2^\mu k_3^\rho \\ &\quad \left. - \frac{28}{45} k_1^\nu k_2^\lambda k_3^\mu k_3^\rho + \frac{4}{15} k_1^\lambda k_2^\mu k_2^\nu k_3^\rho + \frac{28}{45} k_1^\nu k_2^\mu k_3^\lambda k_3^\rho \right] \end{aligned}$$

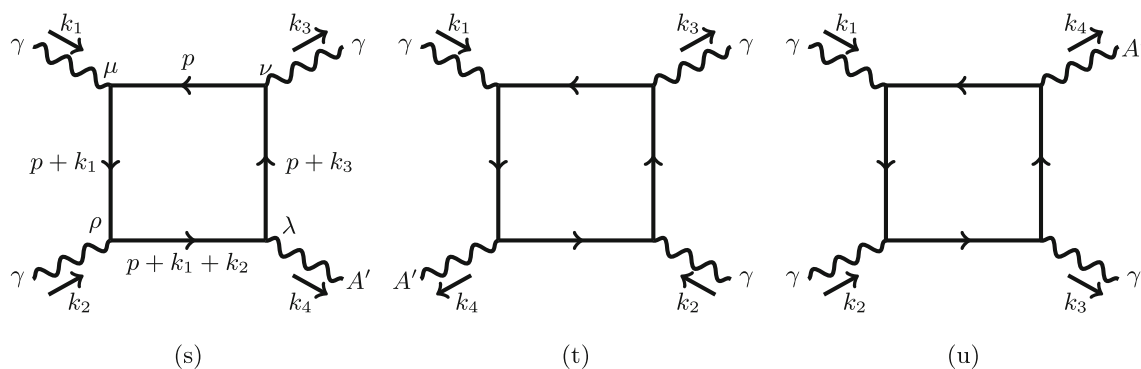


Fig. 1 Three Feynman diagrams of $\gamma\gamma \rightarrow \gamma A'$, the other three differ from these only in that the internal electron loop is traversed in the opposite direction. Amplitude of the diagram with clockwise loop current gives the same contribution with anticlockwise current case

$$\begin{aligned}
 & -\frac{4}{15}k_1^\nu k_2^\lambda k_3^\mu k_3^\rho - \frac{4}{15}k_1^\lambda k_2^\nu k_3^\mu k_3^\rho \\
 & + \frac{28}{45}(m_{A'}^2 - s - t)k_1^\rho k_1^\nu g^{\lambda\mu} - \frac{28}{45}tk_1^\rho k_2^\nu g^{\lambda\mu} \\
 & + \frac{28}{45}sk_1^\nu k_3^\rho g^{\lambda\mu} - \frac{2}{15}(s + t)k_2^\nu k_3^\rho g^{\lambda\mu} \\
 & - \frac{28}{45}(m_{A'}^2 - s - t)k_1^\nu k_2^\mu g^{\lambda\rho} + \frac{28}{45}tk_2^\mu k_2^\nu g^{\lambda\rho} \\
 & - \frac{2}{15}(m_{A'}^2 - t)k_1^\nu k_3^\mu g^{\lambda\rho} + \frac{28}{45}sk_2^\nu k_3^\mu g^{\lambda\rho} \\
 & + \frac{2}{15}(m_{A'}^2 - s)k_1^\rho k_2^\mu g^{\lambda\nu} + \frac{28}{45}sk_3^\mu k_3^\rho g^{\lambda\nu} \\
 & + \frac{28}{45}tk_2^\mu k_3^\rho g^{\lambda\nu} + \frac{28}{45}(m_{A'}^2 - s - t)k_1^\rho k_1^\mu g^{\lambda\nu} \\
 & - \frac{14}{45}(m_{A'}^2 - s - t)k_1^\lambda k_1^\nu g^{\mu\rho} \\
 & + \frac{14}{45}(m_{A'}^2 - s - t)k_1^\nu k_2^\lambda g^{\mu\rho} + \frac{14}{45}tk_1^\lambda k_2^\nu g^{\mu\rho} \\
 & - \frac{14}{45}tk_2^\lambda k_2^\nu g^{\mu\rho} - \frac{2}{45}(3s - 7t)k_2^\nu k_3^\lambda g^{\mu\rho} \\
 & + \frac{2}{45}(7m_{A'}^2 - 10s - 7t)k_1^\nu k_3^\lambda g^{\mu\rho} \\
 & - \frac{14}{45}(m_{A'}^2 - s - t)k_1^\lambda k_1^\rho g^{\mu\nu} - \frac{14}{45}sk_1^\lambda k_3^\rho g^{\mu\nu} \\
 & + \frac{1}{45}(-3m_{A'}^2s + 3s^2 + 14m_{A'}^2t - 14st - 14t^2)g^{\lambda\nu}g^{\mu\rho} \\
 & - \frac{14}{45}(m_{A'}^2 - s - t)k_1^\rho k_3^\lambda g^{\mu\nu} \\
 & - \frac{2}{45}(7m_{A'}^2 - 7s - 10t)k_1^\rho k_2^\lambda g^{\mu\nu} \\
 & + \frac{1}{45}(14m_{A'}^2s - 14s^2 - 3m_{A'}^2t - 14st + 3t^2)g^{\lambda\rho}g^{\mu\nu} \\
 & + \frac{2}{45}(7s - 3t)k_2^\lambda k_3^\rho g^{\mu\nu} - \frac{14}{45}sk_3^\lambda k_3^\rho g^{\mu\nu} \\
 & - \frac{14}{45}tk_2^\lambda k_2^\mu g^{\rho\nu} - \frac{14}{45}tk_2^\mu k_3^\lambda g^{\rho\nu} - \frac{14}{45}sk_2^\lambda k_3^\mu g^{\rho\nu} \\
 & + \frac{2}{45}(3m_{A'}^2 - 3s - 10t)k_1^\lambda k_2^\mu g^{\rho\nu} \\
 & - \frac{2}{45}(3m_{A'}^2 - 10s - 3t)k_1^\lambda k_3^\mu g^{\rho\nu} - \frac{14}{45}sk_3^\lambda k_3^\mu g^{\rho\nu} \\
 & + \frac{1}{45}(-3m_{A'}^2s + 3s^2 - 3m_{A'}^2t + 20st + 3t^2)g^{\lambda\mu}g^{\rho\nu} \Big]. \tag{11}
 \end{aligned}$$

Therefore the amplitude square is:

$$|\mathcal{M}_{\text{fi}}|^2 = \left(\frac{i\varepsilon e^4}{16\pi^2} \right)^2 \frac{1}{4} |\Pi|^2 \tag{12}$$

where $\frac{i}{16\pi^2}$ comes from normalization in loop integration, and $1/4$ comes from the average over initial spins.

Take $e = \sqrt{\alpha 4\pi}$, $t = \frac{s - m_{A'}^2}{2}(\cos\theta - 1)$, Eq. (12) and $\alpha^2 = r_e^2 m^2$ into Eq. (5), differential cross section becomes:

$$\begin{aligned}
 \frac{d\sigma}{d\Omega} = & -\frac{\varepsilon^2 r_e^2 \alpha^2 (m_{A'}^2 - 4\omega^2)^3}{33177600\pi^2 \omega^4 m^6} (139m_{A'}^4 + 968m_{A'}^2 \omega^2 \\
 & + 20016\omega^4 - 278m_{A'}^4 \cos^2\theta + 144m_{A'}^2 \omega^2 \cos^2\theta \\
 & + 13344\omega^4 \cos^2\theta + 139m_{A'}^4 \cos^4\theta \\
 & - 1112m_{A'}^2 \omega^2 \cos^4\theta + 2224\omega^4 \cos^4\theta). \tag{13}
 \end{aligned}$$

Angular distribution of this reaction is shown in Fig. 2. Take limit $\varepsilon \rightarrow 1$, $m_{A'} \rightarrow 0$, Eq. (13) could go back to the case of photon-photon scattering in textbook [45].

3 Background analysis and constraints

In the center-of-mass system, kinetic analysis indicates final state photon and dark photon carry energies of $\omega - \frac{m_{A'}^2}{4\omega}$ and $\omega + \frac{m_{A'}^2}{4\omega}$ respectively. $\omega = 0.5$ MeV, $m_{A'} < 1$ MeV. Therefore the signal we need to search is monophoton with energy less than 0.5 MeV plus the missing energy.

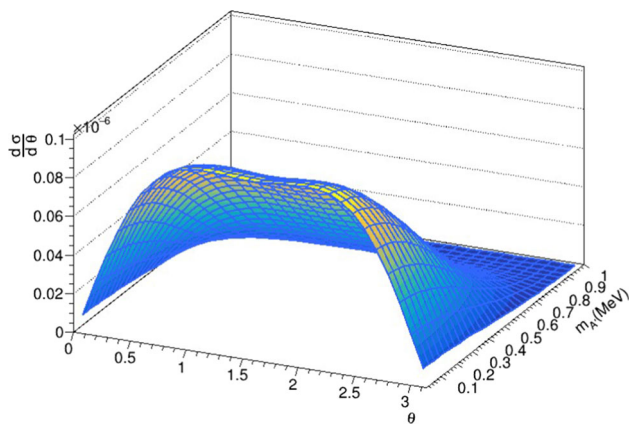


Fig. 2 Angular distribution of reaction $\gamma\gamma \rightarrow \gamma A'$ (take $\varepsilon = 1$). θ is the angle between directions of outgoing and incoming photons, and dark photon is considered with mass range $m_{A'} < 1$ MeV

As a simplification of the discussion, the detector efficiency is assumed to be 1, which means any final state photon that could travel into the detector can be detected. Taken into account of shape of the detector, final state photons that can get into the detector must satisfy $|\cos \theta| < 0.8944$ [46], where θ is the angle between directions of outgoing photon and incoming photon.

In a γ - γ collider, following processes may happen [46]:

- Scattering of light-by-light: $\gamma\gamma \rightarrow \gamma\gamma$.
- Breit–Wheeler process as well as cases with final state radiations: $\gamma\gamma \rightarrow e^+e^-$, $\gamma\gamma \rightarrow e^+e^-\gamma$, $\gamma\gamma \rightarrow e^+e^-\gamma\gamma$.
- Compton scattering of a Compton photon and a beam electron: $e^-\gamma \rightarrow e^-\gamma$.
- Möller scattering of beam electrons: $e^-e^- \rightarrow e^-e^-$.

The initial photon energy is set to be 0.5 MeV, which means under this energy scale, electron positron pair could only appear as virtual states, therefore the Breit–Wheeler processes are out of our consideration. On the other hand, beam electron has energy about 200 MeV, outgoing photons of this ultra-relativistic Compton scattering has very small θ , so most of Compton photons could not travel into the detector. Hence this process is not taken into consideration as well.

Therefore only scattering of light-by-light is considered as the background. $\frac{S}{\sqrt{S+B}} > 1.64$ is set to give the 95% C.L. constraint. Here S and B are signal and background events respectively. The luminosity of γ - γ collider is taken as $L = 4 \times 10^{27} \text{ cm}^{-2} \text{ s}^{-1}$ [46]. Four time scales are considered: 6 months, 1 year, 3 years and 5 years. Constraints for each time interval are given in Fig. 3, in which orange solid line is limit with 5-years' run-time of γ - γ collider. The other three, green dot line, brown dot dashed line and blue dashed line are considered under 3-years', 1-year' and 6-months' collider

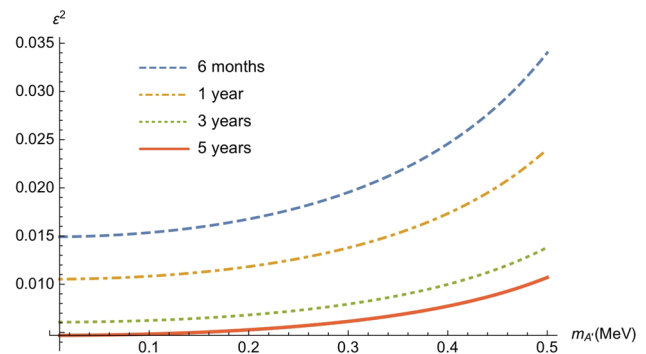


Fig. 3 Limits on dark photon from γ - γ collider. Orange solid line is constraint with γ - γ collider has a run-time of 5 years. The other three, blue dashed line is considered under 6-months' run-time, brown dot dashed line is of 1-year operation and green dot line is 3 years

run-time respectively. Obviously we can see that longer time scale gives more stringent constraint on dark photon.

Current limits on massive dark photon for $m_{A'} < 1$ MeV mainly come from cosmology, astrophysics, atomic experiments, XENON10, TEXONO, etc. COBE/FIRAS gives constraints on dark photon by measuring the distortions of the CMB spectrum, kinetic mixing parameter $\varepsilon \geq 10^{-4}$ are excluded in mass window $10^{-15} \sim 10^{-11}$ eV [47]. Constraints on solar hidden photon are given by CAST [48] and SHIPS [49]. There are also limits from solar lifetime (SUN-T, SUN-L), red giants (RG) and horizontal branches (HB) [50]. In atomic experiments, dark photons are constrained by the sensitive test of Coulomb's law on atomic length scales [51].

4 Summary

In this work, the feasibility of searching dark photon in γ - γ collider is considered. With PACKAGE-X, differential cross section of process $\gamma\gamma \rightarrow \gamma A'$ is calculated. For the simplicity of discussion, any final state photon with $|\cos \theta| < 0.8944$ are assumed to be detected. Taken scattering of light-by-light as background, constraints are given with different time intervals of 6 months, 1 year, 3 years and 5 years, as shown in Fig. 3.

Compared with other constraints on dark photon lighter than 1 MeV, the upper limit of dark photon in a γ - γ collider is not as stringent as others. This is probably restricted to the capability of the machine, which could not offer higher luminosity under current level of technology. We can expect as energy and luminosity increase in a future γ - γ collider, it will be able to detect a wider dark photon mass window and give better limits.

Acknowledgements I would like to thank C.Y.Gao, X.Guan, Y.D.Liu and H.Zhang for useful discussions. This work is supported in part by National Natural Science Foundation of China (11655003); Innovation

Project of IHEP (542017IHEPZZBS11820, 542018IHEPZZBS12427); the CAS Center for Excellence in Particle Physics (CCEPP).

Data Availability Statement This manuscript has no associated data or the data will not be deposited. [Authors' comment: There are no associated data available.]

Open Access This article is licensed under a Creative Commons Attribution 4.0 International License, which permits use, sharing, adaptation, distribution and reproduction in any medium or format, as long as you give appropriate credit to the original author(s) and the source, provide a link to the Creative Commons licence, and indicate if changes were made. The images or other third party material in this article are included in the article's Creative Commons licence, unless indicated otherwise in a credit line to the material. If material is not included in the article's Creative Commons licence and your intended use is not permitted by statutory regulation or exceeds the permitted use, you will need to obtain permission directly from the copyright holder. To view a copy of this licence, visit <http://creativecommons.org/licenses/by/4.0/>.

Funded by SCOAP³.

References

1. V. Trimble, Existence and nature of dark matter in the universe. *Annu. Rev. Astron. Astrophys.* **25**, 425–472 (1987)
2. V. Trimble, History of dark matter in galaxies. *Planets Stars Stellar Syst.* **5**, 1091 (2013)
3. J. De Swart, G. Bertone, J. van Dongen, How dark matter came to matter. *Nat. Astron.* **1**(3), 1–9 (2017)
4. G. Bertone, D. Hooper, History of dark matter. *Rev. Mod. Phys.* **90**(4), 045002 (2018)
5. J.C. Kapteyn, First attempt at a theory of the arrangement and motion of the sidereal system. *Astrophys. J.* **55**, 302 (1922)
6. F. Zwicky, Die rotverschiebung von extragalaktischen nebeln. *Helv. Phys. Acta* **6**, 110–127 (1933)
7. V.C. Rubin, W.K. Ford Jr., N. Thonnard, Rotational properties of 21 SC galaxies with a large range of luminosities and radii, from NGC 4605(R = 4 kpc) to UGC 2885(R = 122 kpc). *Astrophys. J.* **238**, 471–487 (1980)
8. E. Corbelli, P. Salucci, The extended rotation curve and the dark matter halo of M33. *Mon. Not. R. Astron. Soc.* **311**(2), 441–447 (2000)
9. A. Bosma, 21-cm line studies of spiral galaxies. II. The distribution and kinematics of neutral hydrogen in spiral galaxies of various morphological types. *Astron. J.* **86**, 1825–1846 (1981)
10. A. Taylor, S. Dye, T.J. Broadhurst, N. Benitez, E. Van Kampen, Gravitational lens magnification and the mass of Abell 1689. *Astrophys. J.* **501**(2), 539 (1998)
11. P. Natarajan, U. Chadayammuri, M. Jauzac, J. Richard, J.-P. Kneib, H. Ebeling, F. Jiang, F. Van Den Bosch, M. Limousin, E. Jullo et al., Mapping substructure in the HST Frontier Fields cluster lenses and in cosmological simulations. *Mon. Not. R. Astron. Soc.* **468**(2), 1962–1980 (2017)
12. D. Clowe, M. Bradač, A.H. Gonzalez, M. Markevitch, S.W. Randall, C. Jones, D. Zaritsky, A direct empirical proof of the existence of dark matter. *Astrophys. J. Lett.* **648**(2), L109 (2006)
13. E. Komatsu, K.M. Smith, J. Dunkley, C.L. Bennett, B. Gold, G. Hinshaw, N. Jarosik, D. Larson, M.R. Nolta, L. Page et al., Seven-year Wilkinson microwave anisotropy probe (WMAP) observations: cosmological interpretation. *Astrophys. J. Suppl. Ser.* **192**, 18 (2011)
14. P.A. Ade, N. Aghanim, C. Armitage-Caplan, M. Arnaud, M. Ashdown, F. Atrio-Barandela, J. Aumont, C. Baccigalupi, A.J. Bandy, R. Barreiro et al., Planck 2013 results. XVI. Cosmological parameters. *Astron. Astrophys.* **571**, A16 (2014)
15. R.J. Scherrer, M.S. Turner, On the relic, cosmic abundance of stable, weakly interacting massive particles. *Phys. Rev. D* **33**(6), 1585 (1986)
16. D.E. Kaplan, M.A. Luty, K.M. Zurek, Asymmetric dark matter. *Phys. Rev. D* **79**(11), 115016 (2009)
17. R.D. Peccei, H.R. Quinn, Constraints imposed by CP conservation in the presence of pseudoparticles. *Phys. Rev. D* **16**(6), 1791 (1977)
18. K.N. Abazajian et al., Light sterile neutrinos: a white paper (2012). arXiv preprint [arXiv:1204.5379](https://arxiv.org/abs/1204.5379)
19. L.B. Okun, Limits of electrodynamics: paraphotons. Technical report, Gosudarstvennyj Komitet po Ispol'zovaniyu Atomnoj Ehnnergii SSSR (1982)
20. B. Holdom, Searching for ϵ charges and a new U(1). *Phys. Lett. B* **178**(1), 65–70 (1986)
21. B. Holdom, Two U(1)'s and epsilon charge shifts. *Phys. Lett. B* **166**(2), 196–198 (1986)
22. P. Galison, A. Manohar, Two Z's or not two Z's? *Phys. Lett. B* **136**(4), 279–283 (1984)
23. M. Fabbrichesi, E. Gabrielli, G. Lanfranchi, The dark photon (2020). <https://doi.org/10.1007/978-3-030-62519-1>. arXiv preprint [arXiv:2005.01515](https://arxiv.org/abs/2005.01515)
24. S. Gninenko, D. Kirpichnikov, M. Kirsanov, N. Krasnikov, The exact tree-level calculation of the dark photon production in high-energy electron scattering at the CERN SPS. *Phys. Lett. B* **782**, 406–411 (2018)
25. L. Marsicano, M. Battaglieri, M. Bondi, C. Carvajal, A. Celentano, M. De Napoli, R. De Vita, E. Nardi, M. Raggi, P. Valente, Dark photon production through positron annihilation in beam-dump experiments. *Phys. Rev. D* **98**(1), 015031 (2018)
26. P. Fayet, U-boson production in e^+e^- annihilations, ψ and ν decays, and light dark matter. *Phys. Rev. D* **75**(11), 115017 (2007)
27. M. He, X.-G. He, C.-K. Huang, G. Li, Search for a heavy dark photon at future e^+e^- colliders. *J. High Energy Phys.* **2018**(3), 1–20 (2018)
28. P. Ilten, J. Thaler, M. Williams, W. Xue, Dark photons from charm mesons at LHCb. *Phys. Rev. D* **92**(11), 115017 (2015)
29. D. Curtin, R. Essig, S. Gori, J. Shelton, Illuminating dark photons with high-energy colliders. *J. High Energy Phys.* **2015**(2), 157 (2015)
30. S. Gninenko, Search for MeV dark photons in a light-shining-through-walls experiment at CERN. *Phys. Rev. D* **89**(7), 075008 (2014)
31. S. Andreas et al., Proposal for an experiment to search for light dark matter at the SPS (2013). arXiv preprint [arXiv:1312.3309](https://arxiv.org/abs/1312.3309)
32. S. Gninenko, N. Krasnikov, M. Kirsanov, D. Kirpichnikov, Missing energy signature from invisible decays of dark photons at the CERN SPS. *Phys. Rev. D* **94**(9), 095025 (2016)
33. D. Banerjee, V. Burtsev, A. Chumakov, D. Cooke, P. Crivelli, E. Depero, A. Dermenev, S. Donskov, F. Dubinin, R. Dusaev et al., Search for vector mediator of dark matter production in invisible decay mode. *Phys. Rev. D* **97**(7), 072002 (2018)
34. S. Abrahamyan, Z. Ahmed, K. Allada, D. Anez, T. Averett, A. Barbieri, K. Bartlett, J. Beacham, J. Bono, J. Boyce et al., Search for a new gauge boson in electron-nucleus fixed-target scattering by the APEX experiment. *Phys. Rev. Lett.* **107**(19), 191804 (2011)
35. H. Merkel et al., Search at the Mainz Microtron for Light Massive Gauge Bosons Relevant for the Muon g-2 Anomaly. *Phys. Rev. Lett.* **112**(22), 221802 (2014). <https://doi.org/10.1103/PhysRevLett.112.221802>. arXiv preprint [arXiv:1404.5502](https://arxiv.org/abs/1404.5502)
36. J. Lees, V. Poireau, V. Tisserand, E. Grauges, A. Palano, G. Eigen, D.N. Brown, M. Derdzinski, A. Giuffrida, Y.G. Kolomensky et al., Search for invisible decays of a dark photon produced in e^+e^- collisions at BaBar. *Phys. Rev. Lett.* **119**(13), 131804 (2017)

37. J. Jiang, H. Yang, C.-F. Qiao, Exploring bosonic mediator of interaction at BESIII. *Eur. Phys. J. C* **79**(5), 1–12 (2019)
38. A. Anastasi et al., Limit on the production of a new vector boson in $e^+e^- \rightarrow u\gamma, u \rightarrow \pi^+\pi^-$ with the KLOE experiment. *Phys. Lett. B* **757**, 356–361 (2016). <https://doi.org/10.1016/j.physletb.2016.04.019>. arXiv preprint [arXiv:1603.06086](https://arxiv.org/abs/1603.06086)
39. K. Andrews, A. Basye, M. Daugherty, D. Isenhower, T. Jones, D. Jumper, A. Miller, R. Pinson, D. Thomas, M. Towell et al., Search for dark photons from neutral meson decays in $p + p$ and $d + Au$ collisions at $\sqrt{s_{NN}} = 200$ GeV. *Phys. Rev. C Nucl. Phys.* **91**(3), 031901 (2015)
40. J.L. Feng, I. Galon, F. Kling, S. Trojanowski, Forward search experiment at the LHC. *Phys. Rev. D* **97**(3), 035001 (2018)
41. I. Hoernig, G. Samach, D. Tucker-Smith, Searching for dilepton resonances below the Z mass at the LHC. *Phys. Rev. D* **90**(7), 075016 (2014)
42. M. Aaboud, G. Aad, B. Abbott, B. Abeloos, S. Abidi, O. AbouZeid, N. Abraham, H. Abramowicz, H. Abreu, R. Abreu et al., Search for new high-mass phenomena in the dilepton final state using 36 fb^{-1} of proton–proton collision data at $\sqrt{s} = 13$ TeV with the ATLAS detector. *J. High Energy Phys.* **2017**(10), 1–61 (2017)
43. J. Gronberg, The photon collider. *Rev. Accel. Sci. Technol.* **7**, 161–175 (2014)
44. H.H. Patel, Package-X: a mathematica package for the analytic calculation of one-loop integrals. *Comput. Phys. Commun.* **197**, 276–290 (2015)
45. V. Berestetskii, E. Lifshitz, V. Pitaevskii, *Relativistic quantum theory*. pt. 2. Course of theoretical physics—Pergamon International Library of Science, p. 489 (1974)
46. T. Takahashi, G. An, Y. Chen, W. Chou, Y. Huang, W. Liu, W. Lu, J. Lv, G. Pei, S. Pei et al., Light-by-light scattering in a photon–photon collider. *Eur. Phys. J. C* **78**(11), 1–7 (2018)
47. A.A. Garcia, K. Bondarenko, S. Ploekinger, J. Pradler, A. Sokolenko, Effective photon mass and (dark) photon conversion in the inhomogeneous universe. *J. Cosmol. Astropart. Phys.* **2020**(10), 011 (2020)
48. J. Redondo, Helioscope bounds on hidden sector photons. *J. Cosmol. Astropart. Phys.* **2008**(07), 008 (2008)
49. M. Schwarz, E.-A. Knabbe, A. Lindner, J. Redondo, A. Ringwald, M. Schneide, J. Susol, G. Wiedemann, Results from the solar hidden photon search (SHIPS). *J. Cosmol. Astropart. Phys.* **2015**(08), 011 (2015)
50. H. An, M. Pospelov, J. Pradler, New stellar constraints on dark photons. *Phys. Lett. B* **725**(4–5), 190–195 (2013)
51. J. Jaeckel, S. Roy, Spectroscopy as a test of Coulomb’s law: a probe of the hidden sector. *Phys. Rev. D* **82**(12), 125020 (2010)